

# Gas Permeability of Crosslinked HTPB-H<sub>12</sub>MDI-Based Polyurethane Membrane

SHIH-LIANG HUANG and JUIN-YIH LAI\*

Chemical Engineering Department, Chung Yuan University, Chung Li, Taiwan, 32023 Republic of China

## SYNOPSIS

Crosslinked membranes were prepared by the addition of a crosslinking agent of benzoyl peroxide (BPO) to the hydroxyl-terminated polybutadiene (HTPB) and 4,4'-dicyclohexylmethane diisocyanate (H<sub>12</sub>MDI)-based polyurethane (PU) solutions. The stress-strain properties of segmented HTPB-based PUs were changed by the crosslinking between soft-soft segments. The gas permeabilities of HTPB-based PU membranes with a suitable amount of crosslinking agent were higher than those of uncrosslinked membranes, which is due to the stretched and extended soft-segment molecular chains. The reproducibility of gas permeability was improved by the crosslinked membranes. Thermal stability conducted by TGA was increased with increasing crosslinking agent content. FTIR was utilized to identify the segregation between hard and soft segments and structure change, which affects the gas-transport properties. The change of glass transition temperature was detected by DSC, which can be used to manifest the degree of crosslinking of these membranes. The results of TGA, FTIR, and DSC measurements explain the crosslinking degree with different BPO content and, hence, the gas permeabilities as well. © 1995 John Wiley & Sons, Inc.

## INTRODUCTION

Hydroxyl-terminated polybutadiene (HTPB)-based polyurethanes (PUs) can be used for gas separation because of their low-temperature flexibility and the high segregation between hard and soft segments due to the nonpolarity of the HTPB segment. 4,4'-Dicyclohexylmethane diisocyanate (H<sub>12</sub>MDI) is a viscous liquid, which is easy to use for the synthesis of PU polymers and the preparation of membranes.

The crosslinking of PU polymers was generally obtained by the introduction of diol and triol mixtures to the PU prepolymer.<sup>1,2</sup> Don et al.<sup>3</sup> reported that the chain scission reaction and crosslinking appeared to be due to the thermal energy in the annealing behavior of HTPB-methane diisocyanate (MDI)-based PU at 80°C. Yoshikawa et al.<sup>4</sup> studied the crosslinking of polybutadiene (PB) membranes arising from the chemical reactions with the crosslinking agent of bis(1-methyl-1-phenyl-ethyl)peroxide at the sites of unsaturation in the polymer chain. This study at-

tempts to prepare the crosslinked HTPB-based PU membranes by using benzoyl peroxide (BPO) to crosslink between soft and soft segments of butadiene.

The gas permeability property and its relationship with HTPB/H<sub>12</sub>MDI/1,4-BD compositions and the crosslinking agent content at various temperatures were investigated in this study. The different stress and strain properties between crosslinked and uncrosslinked membranes were studied also. DSC and TGA were used to study the change of glass transition temperature and thermal decomposition characteristics. Hydrogen-bonding index (HBI) values for the indication of phase segregation were measured by FTIR. The measurements of DSC, TGA, and FTIR were used to identify the degree of crosslinking and, hence, to correlate the gas permeabilities with different crosslinking agent content.

## EXPERIMENTAL

### Materials

The chemicals used for this study were 4,4'-dicyclohexylmethane diisocyanate (H<sub>12</sub>MDI, Desmodur

\* To whom correspondence should be addressed.

W of Mobay Co.), hydroxyl-terminated polybutadiene (HTPB, equivalent weight 1370 g, average functionality of 2.3, R-45M of ARCO Co.), 1,4-butanediol (1,4-BD) as a chain extender, and dibutyltin dilaurate (DBTDL) as a catalyst. Benzoyl peroxide (BPO) was used as a crosslinking agent.

### Preparation of Polyurethane Membrane

The two-stage PUs were polymerized first by a —NCO terminated prepolymer and then chain-extended with 1,4-BD under 25 wt % solid content after theoretical —NCO content was reached. It was diluted to a 15 wt % solid content after the chain-extended reaction proceeded for 30 min. The reaction was terminated as the —NCO groups were completely consumed, as confirmed by the disappearance of the infrared (IR) absorption at  $2280\text{ cm}^{-1}$ .

Uncrosslinked membranes were prepared by pouring the solution mixture onto a glass plate to a thickness of  $600\text{ }\mu\text{m}$ . The solvent in the casting solution was evaporated by degassing at  $50^\circ\text{C}$  for 24 h. The dried PU membranes were peeled from the plate after it had been immersed in deionized water for several hours. The PU membranes were dried in a desiccator and stored at a relative humidity of 50% and  $25^\circ\text{C}$  for 5 days before property testing.

Crosslinked membranes were prepared by adding 0.5, 1.0, and 2.0 wt % (based on solid PU content) of BPO to the PU solution (15 wt % solid content) in the closed vessel at  $60^\circ\text{C}$  for 6 h. All the following membrane preparation steps were the same as that of uncrosslinked membranes. Types of different compositions in this study are shown by symbol L, M, and H, which individually represent the equivalent ratio of HTPB/ $\text{H}_{12}$ MDI/1,4-BD = 1/4/3, 1/8/7, and 1/12/11. Numbers of 0, 0.5, 1.0, and 2.0 represent that the above PU compositions are crosslinked by 0, 0.5, 1.0, and 2.0 wt % of BPO, respectively.

### Gas Permeation Measurement

Oxygen and nitrogen permeabilities of membranes were determined by using the Yanaco GTR-10 gas permeability analyzer. A detailed procedure for measuring the gas permeation was reported in a previous publication.<sup>5</sup> The gas permeability was determined by the following equation:

$$P = \frac{q \cdot l}{(p_1 - p_2) \cdot A \cdot t}$$

where  $P$  is the gas permeability [ $\text{cm}^3$  (STP)  $\text{cm}^2$

$\text{cm}^2\text{ s cmHg}$ ];  $q/t$ , the volumetric flow rate of gas permeation [ $\text{cm}^3$  (STP)/ $\text{s}$ ];  $l$ , the membrane thickness (cm);  $p_1$  and  $p_2$ , the pressures (cmHg); and  $A$ , the effective membrane area ( $\text{cm}^2$ ).

### Properties Measurement

Stress-strain testing was performed according to the ASTM D412 standard method at a crosshead speed of  $50\text{ cm/min}$ , with a clamp distance of 3 in. A DuPont 9000 instrument was used for DSC measurement, using liquid nitrogen for cooling and with a heating rate of  $10^\circ\text{C/min}$  in the temperature range between  $-120$  and  $150^\circ\text{C}$ . A Bio-Rad FTS-7 was used for the infrared spectra measurement. A DuPont 951 instrument was used for the TGA measurement with a heating rate of  $20^\circ\text{C/min}$  in the temperature range from  $50$  to  $600^\circ\text{C}$ .

### Crosslinking Reaction

BPO was decomposed first and an active site was produced by capturing the hydrogen atom nearing the double bonds of the HTPB soft segment as shown in Figure 1. This active site then reacted with other HTPB chains with or without an active site.<sup>4</sup> Then, the crosslinkage between HTPB soft segments was formed.

## RESULTS AND DISCUSSION

### Crosslinking and Temperature Effect

Figures 2–4 show that gas permeabilities are all increased as the temperature increased. The gas per-

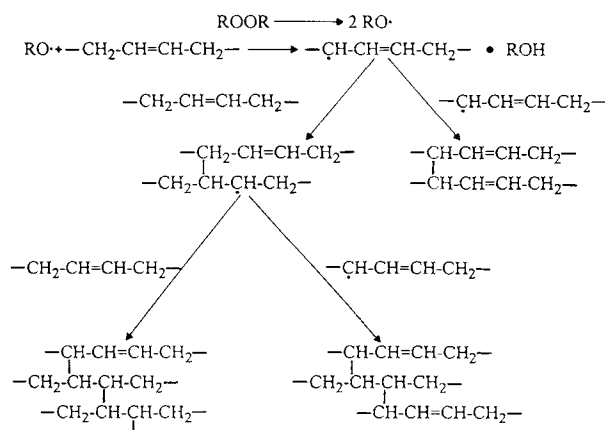


**Figure 1** Crosslinking reactions of soft-segment HTPB. (The figure was abstracted from Yoshikawa et al.<sup>4</sup>)

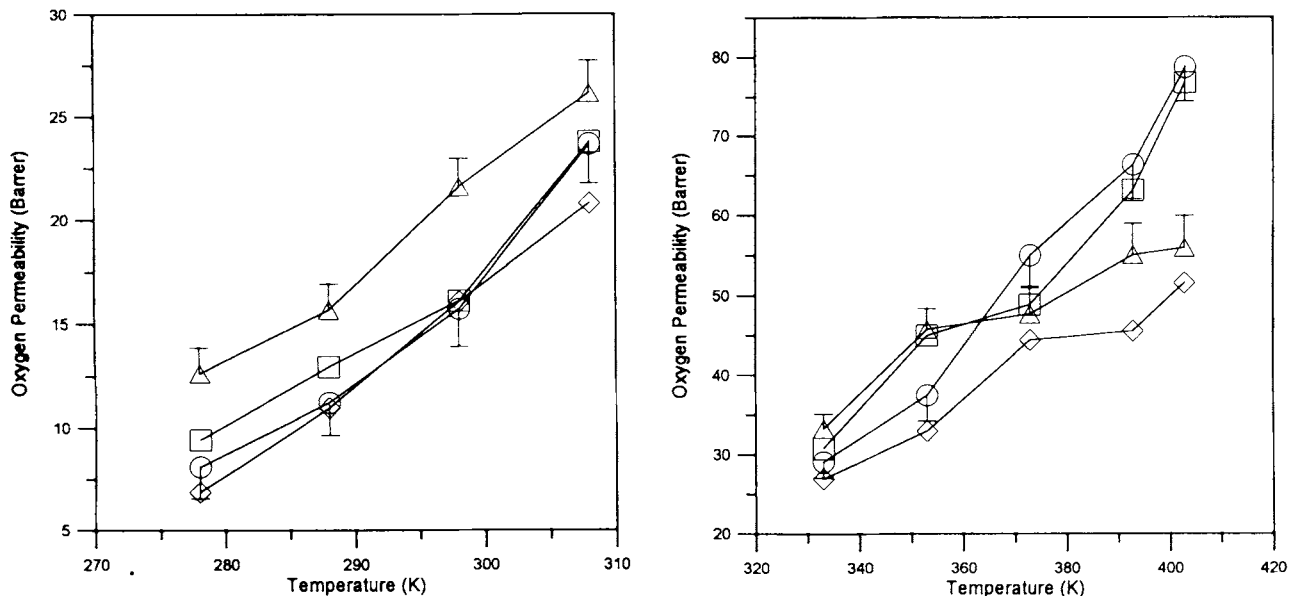


**Figure 2** Effect of temperature on the gas permeability of HTPB/H<sub>12</sub>MDI/1,4-BD = 1/4/3 with (○) 0.0, (□) 0.5, (△) 1.0, and (◇) 2.0 wt % of BPO content, respectively.

meabilities of membranes with a suitable amount of BPO content were slightly higher than those of uncrosslinked ones, whereas the separation factors remain nearly constant for any composition of cross-linked and uncrosslinked membranes at any temperature. Nitrogen permeability also increases with a suitable amount of crosslinking agent. The domain structure in segmented urethanes is an unstable morphology with respect to temperature.<sup>6</sup> Figure 5

shows that the degree of domain formation of uncrosslinked PU apparently decreases upon heating and the domain structure was suggested to reform upon cooling. For the crosslinked PU, the soft segments were crosslinked to each other. These molecular chains of the soft segment will be more extended and stretched tightly. This could be explained by that the coiled molecular chain of the soft segment was stretched as the BPO content increased and the

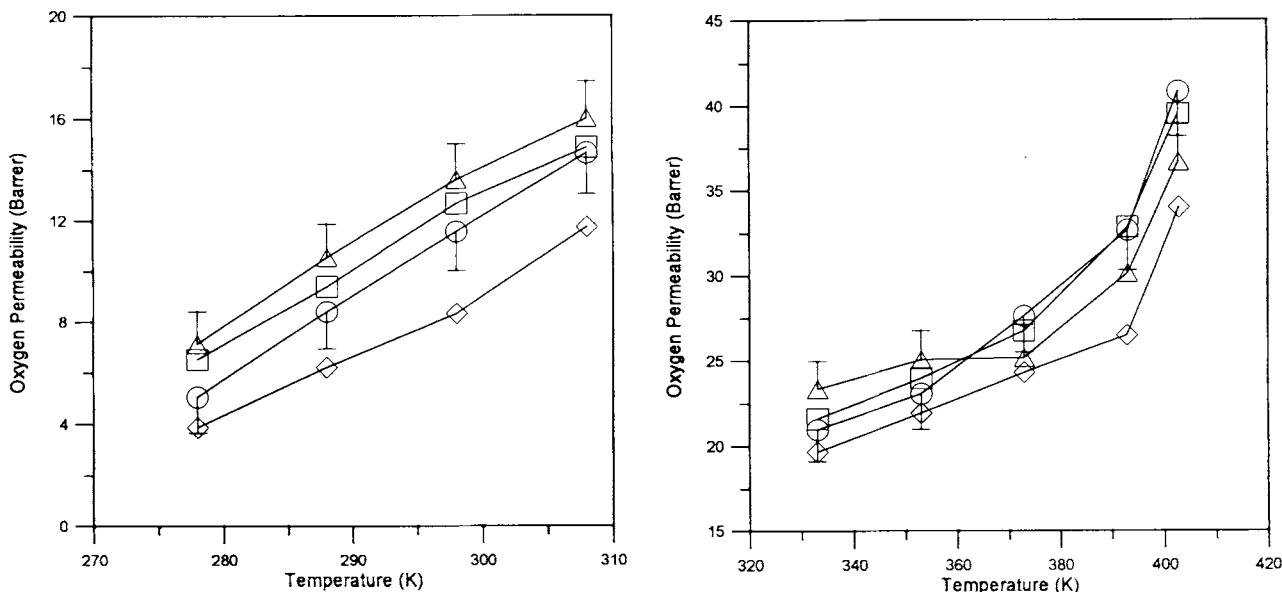


**Figure 3** Effect of temperature on the gas permeability of HTPB/H<sub>12</sub>MDI/1,4-BD = 1/8/7 with (○) 0.0, (□) 0.5, (△) 1.0, and (◇) 2.0 wt % of BPO content, respectively.

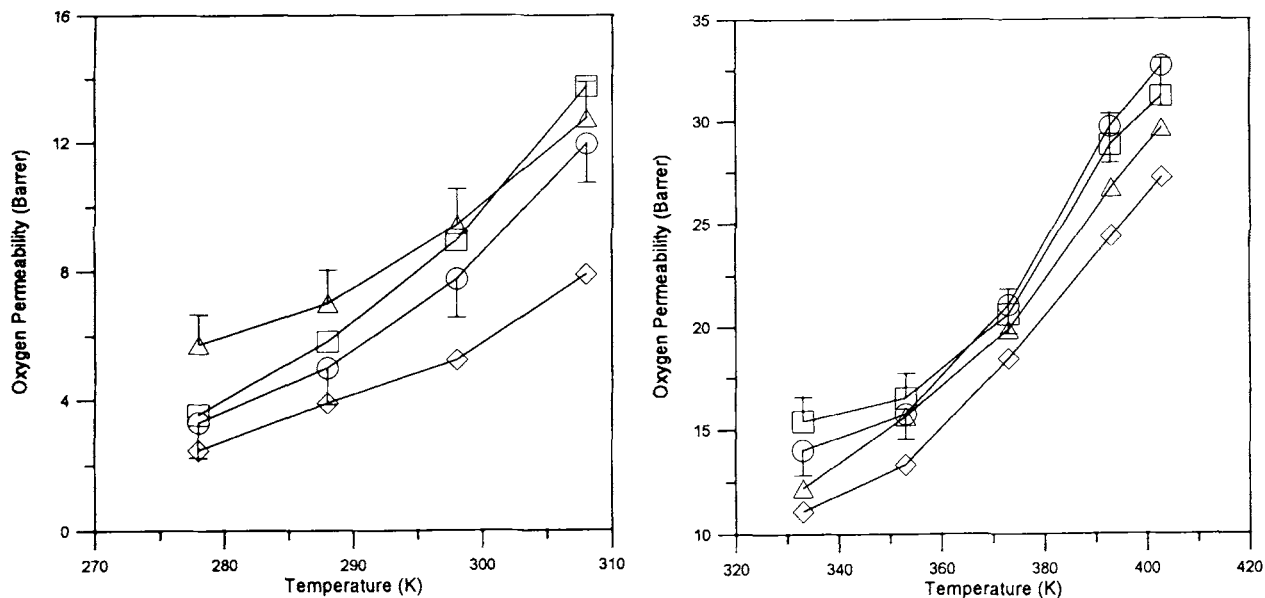


**Figure 4** Effect of temperature on the gas permeability of HTPB/H<sub>12</sub>MDI/1,4-BD = 1/12/11 with (○) 0.0, (□) 0.5, (△) 1.0, and (◇) 2.0 wt % of BPO content, respectively.

interchain spacing increased as the temperature increased. Measurements of gas permeabilities of crosslinked membranes exhibited higher reproducibility than did those of uncrosslinked membranes. Owing to the higher crosslinkage between soft-soft segments, the gas permeability of the membrane with a BPO content of 2.0 wt % is lower than that of the uncrosslinked membranes. The degrees of crosslinkage with different BPO content can be identified by a wavenumber shiftment of about 2–5  $\text{cm}^{-1}$ , as shown in Table I and a change of 2–7°C of two glass transition temperatures, as shown in Table II.

At higher temperature, the gas permeabilities decreased as the BPO content increased. The DSC endotherm in the region of 80°C has been ascribed to the glass transition temperature of the hard segment. The gas permeabilities for membranes with all considered compositions changed sharply from about 80°C, as shown in Figures 2–4. The interchain spacings of crosslinked PU are lower than those that uncrosslinked PUs possess at high temperature. A similar result was reported by Harthcock<sup>7</sup>: that hydrogen bonding between hard-segment domains weakens at about 80°C for PU polymer consisting of six urethane linkage, while the crosslinking structure between soft-soft segments does not. The intermolecular distances increase as the temperature increases.

Higher gas permeabilities of type L membranes were obtained in the considered range of 278–353 K compared to those of uncrosslinked membranes. The

gas permeabilities of type H membranes were observed to be slightly higher than those of uncrosslinked membranes at lower operating temperature. This is due to the higher hard-segment content and higher hydrogen bonding of the hard segment. From this study, it is suggested that the crosslinking effect on the gas permeabilities of membranes are in the order of type L > M > H.

### Infrared Spectroscopy

The polarity difference between nonpolar HTPB soft segment and polar hard segment makes these membranes possess phase segregation. The change of interchain hydrogen bonding was utilized to study the phase segregation. An infrared technique has been found acceptable for measuring the extent of hydrogen bonding.<sup>8,9</sup>

Figure 6 shows that the carbonyl absorption region is between 1800 and 1600  $\text{cm}^{-1}$ , and the carbonyl absorption band splits into two peaks. The peak due to bonded C=O stretching is centered at 1700  $\text{cm}^{-1}$  and that due to free C=O stretching is centered at about 1717  $\text{cm}^{-1}$ . Hydrogen-bonded carbonyl bands will correspond to those groups that are in the interior of hard segments, while the free bands may correspond to those groups in the hard-segment domains or in the soft domains or at the interface.<sup>10</sup> These soft-to-soft segment and soft-to-hard segment interactions can lead to different polymer morphol-

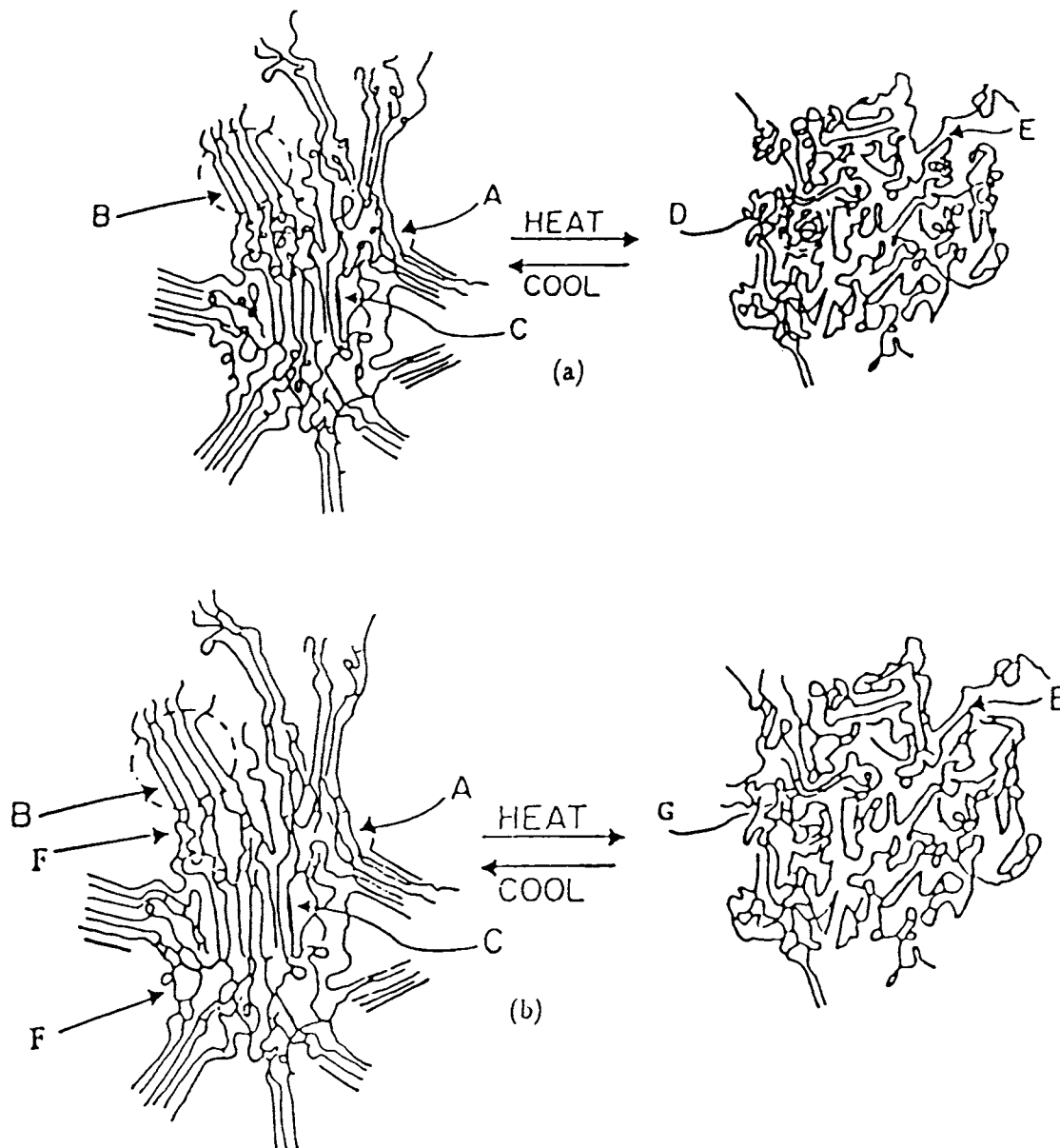


**Figure 5** Schematic model depicting the morphology of (a) uncrosslinked and (b) cross-linked HTPB-based PU. (A) partially extended soft segment; (B) hard-segment domain; (C) hard segment; (D) coiled soft segment; (E) lower-order hard-segment domain; (F) cross-linking of extended soft segment. (The figure was abstracted from Wilkes and Emerson<sup>6</sup> and modified.)

ogies and properties. In the butadiene-containing PUs, hydrogen bonding occurs only between urethane segments of the C=O and N—H groups since the carbonyl in the urethane linkage and the urethane alkoxy oxygen are the only available proton acceptors.

Figure 6 represents the FTIR spectra of the carbonyl stretching for membranes with type L composition from 25 to 120°C. The absorbance of free

carbonyl absorption is increased as the temperature increased and the bonded carbonyl absorption decreased. The extent of the break of hydrogen-bonded carbonyl groups in the hard-segment domain is increased as the temperature increased. For higher temperature, more carbonyl groups were randomly dispersed in the whole polymer chain, inducing the increase of repulsion between polar carbonyl groups and the nonpolar HTPB segment.

**Table I** Wavenumber of Carbonyl Group Absorption

Composition (Equivalent Ratio)	BPO Content (Wt %)	Wavenumber (cm <sup>-1</sup> ) of Bonded Carbonyl Group	Wavenumber (cm <sup>-1</sup> ) of Free Carbonyl Group
HTPB/H12MDI/1,4-BD (1/4/3)	0	1698	1717
	0.5	1698	1717
	1.0	1702	1717
	2.0	1703	1717
HTPB/H12MDI/1,4BD (1/8/7)	0	1695	1713
	0.5	1697	1717
	1.0	1698	1713
	2.0	1702	1716
HTPB/H12MDI/1,4BD (1/12/11)	0	1691	1713
	0.5	1697	1715
	1.0	1697	1715
	2.0	1694	1713

The extent of the carbonyl absorption group participating in hydrogen bonding is expressed by the hydrogen-bonding index (HBI), which is defined as the relative absorbances of the two carbonyl peaks<sup>11</sup>:

$$\text{HBI} = \frac{A_{\text{C=O, bonded}}}{A_{\text{C=O, free}}}$$

where  $A_{\text{C=O, bonded}}$  and  $A_{\text{C=O, free}}$  are, respectively, the absorbance of bonded and free carbonyl groups.

HBI may also be expressed as

$$\text{HBI} = \frac{C_{\text{bonded}} \epsilon_{\text{bonded}}}{C_{\text{free}} \epsilon_{\text{free}}}$$

where  $C$  is the concentration, and  $\epsilon$  the absorption coefficient of carbonyl groups. A number of studies<sup>12,13</sup> have reported that  $\epsilon_{\text{bonded}}/\epsilon_{\text{free}}$  is between 1.0 and 1.2, while 1.71 was used by Coleman et al.<sup>10</sup> Owing to the same diisocyanate (i.e., same chemical structure) of the PU solution and testing temperature, the ratio can assume a constant value. The only interest of this study is the change of the HBI value to indicate the trend of the degree of segregation of the same diisocyanate and temperature.

Table I shows that the extent of wavenumber shiftment increases as the BPO content increases. Upon crosslinking, the energy and force constant of the carbonyl absorption increase and the absorption band is therefore shifted to a higher frequency. The intermolecular hydrogen-bonding shifts the carbonyl absorption to lower frequencies (i.e., the carbonyl absorption frequency decreases), which can be indicated by the higher absorption frequency of 1698

cm<sup>-1</sup> of type L composition to the lower absorption frequency of 1691 cm<sup>-1</sup> of type H composition.

Figure 7 shows that the HBI value decreases as the temperature increases and the HBI values increase in the following BPO content sequence: 2.0 wt % > 0.0 wt % > 0.5 wt % > 1.0 wt %. Hydrogen bonding decreases as the temperature increases, while that of free hydrogen bonding increases. Because of the crosslinking between soft segments at 60°C in the membrane preparation, the carbonyl group of free hydrogen bonding cannot reform new hydrogen bonding upon cooling. The greater HBI values indicate increased participation of the carbonyl group in hydrogen bonding and the lower de-

**Table II** Glass Transition Temperature of PU Membranes

Composition (Equivalent Ratio)	BPO Content (Wt %)	$T_{gs}$ (°C)	$T_{gh}$ (°C)
HTPB/H12MDI/1,4-BD (1/4/3)	0	-74.2	—
	0.5	-70.5	—
	1.0	-66.8	—
	2.0	-67.8	—
HTPB/H12MDI/1,4-BD (1/8/7)	0	-73.7	75.0
	0.5	-71.3	75.0
	1.0	-70.6	77.9
	2.0	-67.6	80.0
HTPB/H12MDI/1,4-BD (1/12/11)	0	-69.3	74.7
	0.5	-67.1	75.0
	1.0	-68.2	75.2
	2.0	-66.8	84.6

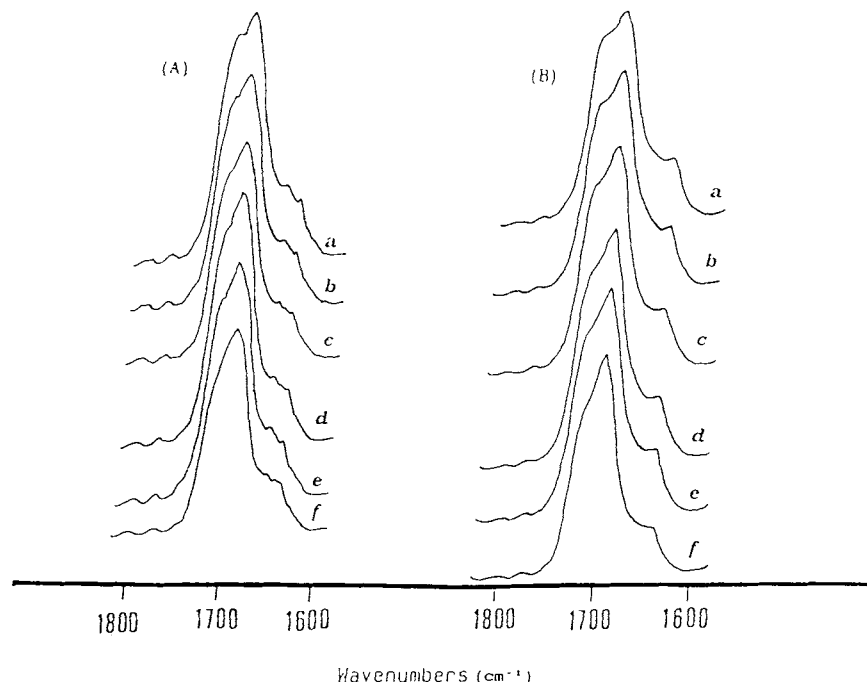


**Figure 6** FTIR spectra of (A) HTPB/H<sub>12</sub>MDI/1,4-BD = 1/4/3, BPO (1.0 wt %) and (B) HTPB/H<sub>12</sub>MDI/1,4-BD = 1/4/3 at different temperatures: (a) 120°C; (b) 100°C; (c) 80°C; (d) 60°C; (e) 35°C; (f) 25°C.

gree of segregation between hard and soft segments. This variation in hydrogen bonding is rather significant for the irregular packing of segments, which increases as the value of HBI decreases. The change of gas permeability with temperature as shown in

Figures 2–4 can be well related to the change of HBI value with temperature.

**Hard Segment Content Effect**

Figure 8 shows that the higher the hard segment content is the lower the gas permeability for all PUs

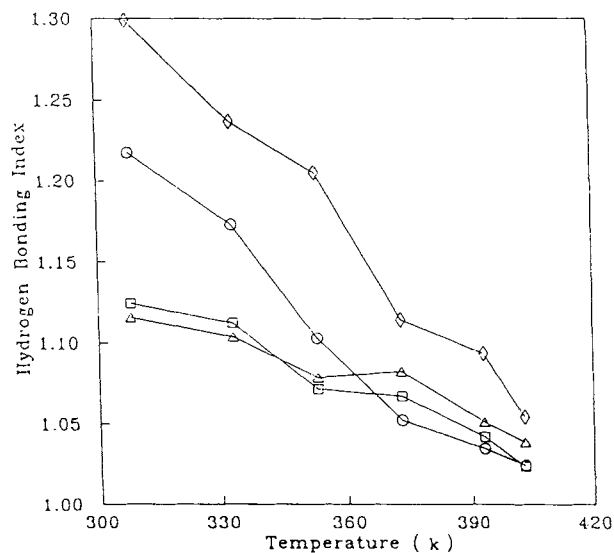


**Figure 7** Effect of temperature on the value of hydrogen-bonding index of HTPB/H<sub>12</sub>MDI/1,4-BD = 1/4/3 with (○) 0.0, (□) 0.5, (△) 1.0, and (◇) 2.0 wt % of BPO content, respectively.

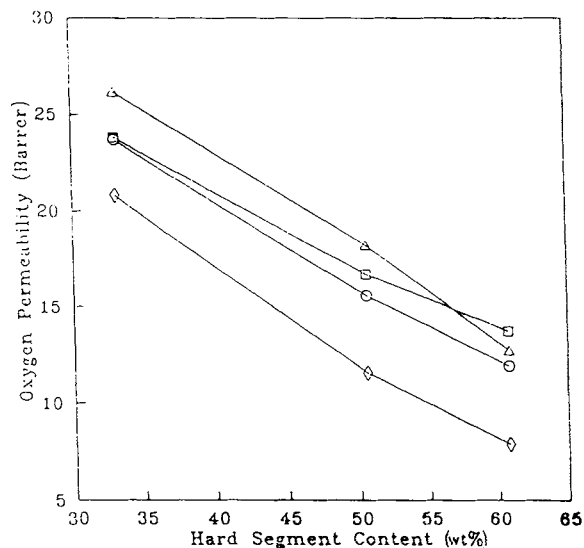


**Figure 8** Effect of hard-segment content on the gas permeability with (○) 0.0, (□) 0.5, (△) 1.0, and (◇) 2.0 wt % of BPO content, respectively.

membranes. These results of HTPB-based PU membranes are contrary to those of conventional polyol-based PU membranes of Hsieh.<sup>14</sup> This could be explained by that more carbonyl groups are hydrogen-bonded in PU membranes with a higher hard-segment content. The segregation between the nonpolar HTPB soft segment and hard segment is decreased, which is due to fewer polar carbonyl groups being freely dispersed in the soft segment. As evidenced, membranes with type M composition possess an HBI of 1.4379, whereas membranes with type L composition possess 1.2176 at 35°C. Landro et al.<sup>15</sup> reported that in the case of PU with a lower polyether chain a larger number of N—H's are available to form hydrogen bonds of C=O and N—H groups between different chains, which may result in a higher ratio of bonded C=O to free C=O.

### Benzoyl Peroxide Content Effect

Figure 9 shows the gas permeabilities of PU membranes with various BPO content. There are maximum gas permeabilities for compositions of types L1.0, M1.0, and H0.5. Higher BPO content is needed to crosslink membranes with lower hard-segment content which possess more unsaturated double bonds. Membranes of composition of types L0.5 and M0.5 have nearly the same gas permeabilities as those of uncrosslinked membranes of the same

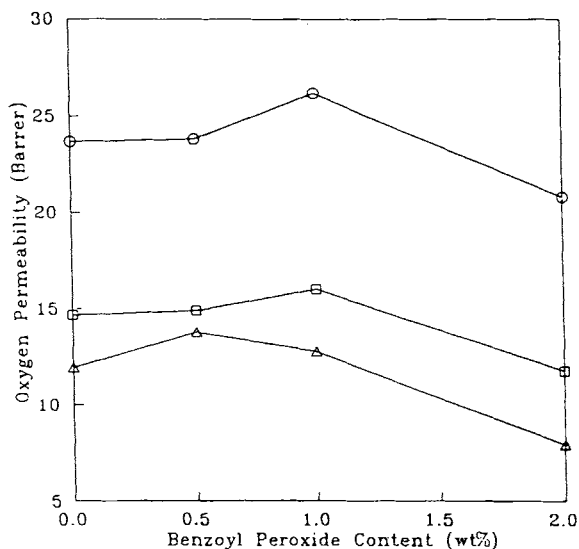


**Figure 9** Effect of BPO content on the gas permeability of (O) HTPB/H<sub>12</sub>MDI/1,4-BD = 1/4/3, (□) HTPB/H<sub>12</sub>MDI/1,4-BD = 1/8/7, and (Δ) HTPB/H<sub>12</sub>MDI/1,4-BD = 1/12/11.

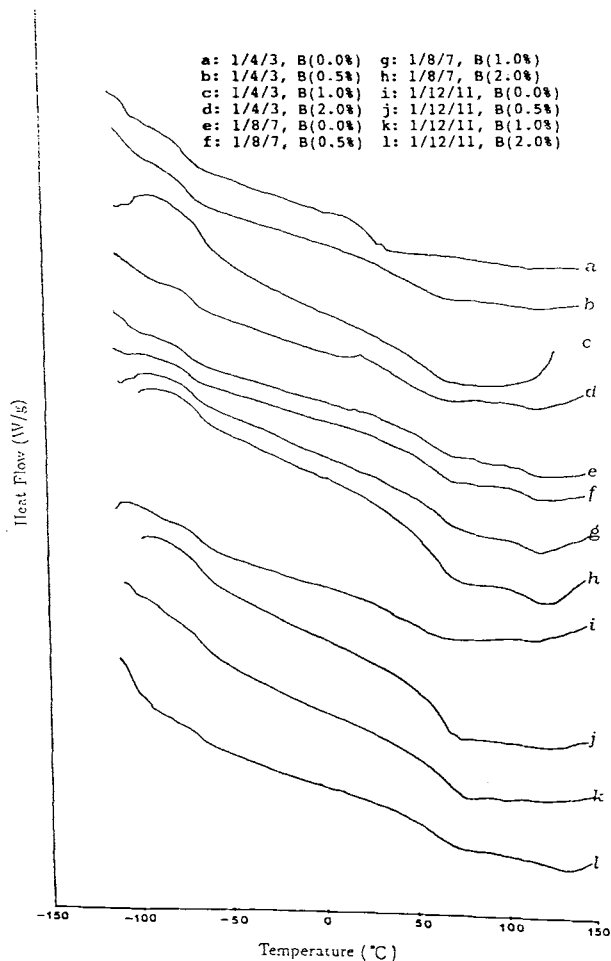


**Figure 10** DSC thermogram of different equivalent ratios of HTPB/H<sub>12</sub>MDI/1,4-BD and weight percentage of BPO content.

compositions, as membranes of all compositions with 2.0 wt % BPO content exhibit lower gas permeabilities due to higher crosslinkage.

### Differential Scanning Calorimeter

Figure 10 presents DSC curves for a number of different hard-segment content membranes as a function of crosslinking agent content. Table II shows that the glass transition temperature of soft segments ( $T_{gs}$ ) and hard segments ( $T_{gh}$ ) increased as the BPO content increased. The  $T_{gh}$  of type L composition cannot be appreciably determined, which is due to the membrane with a lower hard-segment content.<sup>16</sup> The increase of crosslinking by the increase of BPO content increasingly restricts the mobility of the polymer chain and requires more energy for the mobility of the molecular chain.



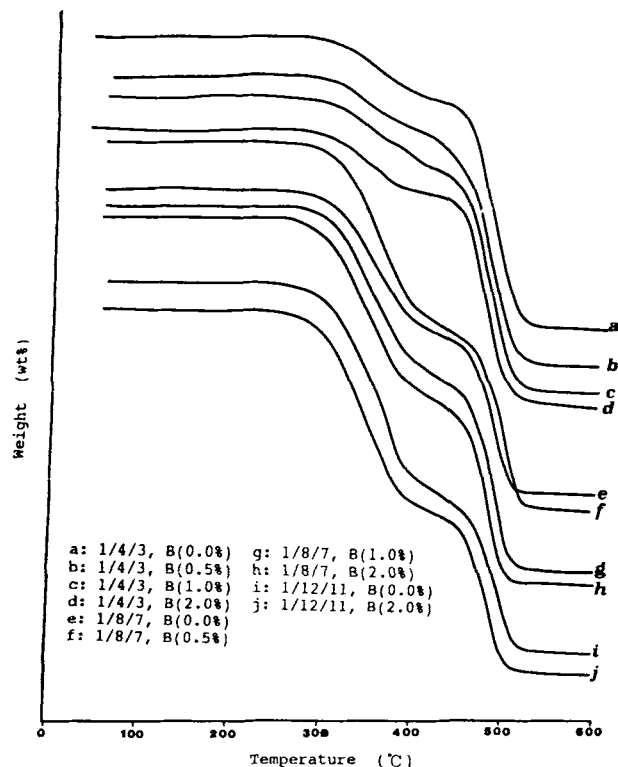


**Figure 11** TGA thermogram of different equivalent ratios of HTPB/H<sub>12</sub>MDI/1,4-BD and weight percentage of BPO content.

### Thermogravimetric Analysis

Thermogravimetric data give quite a good, but only qualitative, indication of the thermal resistance of the material concerned. TGA traces for various HTPB-based PU membranes are reproduced in

Figure 11. A three-step degradation was observed in all these three types of membranes. It is stable up to 300°C and the polymer remains almost intact in the first step. The quantity of gaseous components, mainly water, released in this step is relatively small.

A rapid weight loss starts at approximately 300°C up to 500°C; the main quantity of gaseous components, e.g., water, carbon monoxide, and methane, are split off. Decomposition of step 2 corresponds to the urethane bond breaking and step 3 is the polyol decomposition.<sup>17</sup> In this degradation stage, random chain scission occurs. It can be assumed that a coalescence of chains to form ribbons occurs in this stage.<sup>18</sup> Almost complete decomposition was observed at about 500°C.

Table III shows the decomposition temperature at various weight loss percentages and weight percentage of residue and Step 2 decomposition. Membranes with low hard-segment content have the higher residue and the lower weight loss percentage of step 2 decomposition. Due to the lower oxygen and nitrogen atom content in the molecular structure of lower hard-segment content, these membranes have higher residue remaining after thermogravimetric analysis. The decomposition temperatures of these three types of crosslinked membranes are higher than those of uncrosslinked membranes.

The rates of degradation are much lower for polymers with crosslinkage because of ring formation of the transient species. Crosslinked molecular structures are more thermal resistant than are those of uncrosslinked structures. It has been reported that aromatic ethers usually exhibit good thermal stability<sup>19</sup> and that the thermal stability of IPN of

**Table III** Thermal Behavior of Crosslinked and Uncrosslinked Membranes in Nitrogen Atmosphere

Composition (Equivalent Ratio)	BPO Content (Wt %)	Decomposition Temperature (°C) at Various Wt % Loss					Residue of TGA (Wt %)	Wt % Loss of Second-step Decomposition
		20	40	60	80	90		
HTPB/H <sub>12</sub> MDI/1,4-BD (1/4/3)	0	404	458	477	500	523	9.2	22.5
	0.5	406	463	483	503	527	9.8	22.1
	1.0	402	461	480	500	—	11.5	23.4
	2.0	426	463	482	518	—	14.4	24.4
HTPB/H <sub>12</sub> MDI/1,4-BD (1/8/7)	0	333	382	466	486	495	3.5	50.0
	0.5	350	406	474	494	506	6.8	42.8
	1.0	350	402	471	494	505	7.2	44.9
	2.0	350	398	477	500	511	7.0	47.8
HTPB/H <sub>12</sub> MDI/1,4-BD (1/12/11)	0	321	364	461	489	508	6.0	53.5
	2.0	341	377	461	492	508	6.7	55.4

**Table IV Stress and Strain Measurement of PU Membranes**

Composition (Equivalent Ratio)	BPO Content (Wt %)	Strain at Break (%)	Stress at Break (MPa)
HTPB/H12MDI/1,4-BD (1/4/3)	0	477.0	8.5
	0.5	337.1	11.57
	1.0	310.4	12.29
	2.0	274.8	13.75
HTPB/H12MDI/1,4-BD (1/8/7)	0	203.9	19.86
	0.5	199.4	20.57
	1.0	185.9	21.58
	2.0	178.9	23.69
HTPB/H12MDI/1,4-BD (1/12/11)	0	139.5	24.34
	0.5	124.6	28.18
	1.0	120.4	30.01
	2.0	117.9	32.43

HTPB-based PU and PMMA increased with increasing urethane content, which was crosslinked by glycerol.<sup>2</sup>

Crosslinked PUs have a higher residue than that of uncrosslinked PUs, and PUs with higher BPO content have a higher decomposition temperature and higher weight loss. The reason may be that membranes of tightly crosslinked structures require more energy for the decomposition and ring structure may be formed.

### Stress and Strain Measurements

The effect of crosslinking agent content on the stress and strain behavior of the prepared membranes is shown in Table IV. The stress at break increases as the hard-segment content increases and, on the contrary, the strain at break decreases.<sup>20</sup> The increase of hydrogen bonding of higher hard-segment content results in increase of intermolecular attraction.

In agreement with the FTIR and DSC studies, the stress and strain behavior of these HTPB-based PU membranes was significantly affected by the BPO content. The stress at break of membranes with type L composition are appreciably changed from 8.5 to 13.75 MPa as the composition changes from type L0 to type L2.0. Owing to the lower crosslinkage between soft-soft segments, the stress and strain properties of membranes with higher hard-segment content change slightly, not depending much on the BPO content.

### CONCLUSIONS

Due to the stretched and extended soft-segment molecular chains, HTPB-based PU membranes crosslinked with a suitable amount of BPO content provided higher gas permeability than that of uncrosslinked membranes. Thermal stability was increased with increasing crosslinking agent content. Membranes with higher hard-segment content have lower gas permeability and higher stress strength at break. The stress at break of crosslinked membranes is greatly increased over that of uncrosslinked membranes. The degree of crosslinking can be determined by the change of glass transition temperature and wavenumber shiftment of the carbonyl group. Higher HBI values represent increased participation of the carbonyl group in hydrogen bonding and the lower degree of segregation between hard and soft segments and, hence, the lower gas permeability. The results of TGA, FTIR, and DSC measurements explain the crosslinking degree with different BPO content and, hence, the gas permeabilities well.

The authors thanks the National Science Council of the Republic of China for their financial support (NSC84-2216-E-033-004).

### REFERENCES

1. S. S. Shyu, D. S. Chen, and J. Y. Lai, *J. Appl. Polym. Sci.*, **34**, 2151 (1987).

2. V. Choudhary and R. Gupta, *J. Appl. Polym. Sci.*, **50**, 1075 (1993).
3. T. M. Don, W. Y. Chiu, and K. H. Hsieh, *J. Appl. Polym. Sci.*, **43**, 2193 (1992).
4. M. Yoshikawa, T. Wano, and T. Kitao, *J. Membr. Sci.*, **89**, 23 (1994).
5. J. Y. Lai, J. M. Jen, and S. H. Lin, *Chem. Eng. Sci.*, **48**(24), 4069 (1993).
6. G. L. Wilkes and J. A. Emerson, *J. Appl. Phys.*, **47**(10), 4261 (1976).
7. M. A. Harthcock, *Polymer*, **30**, 1234 (1989).
8. G. A. Senich and W. J. Macknight, *Macromolecules*, **13**(1), 106 (1980).
9. H. S. Lee, Y. K. Wang, and S. L. Hsu, *Macromolecules*, **20**, 2089 (1987).
10. M. M. Coleman, D. J. Skrovanek, J. Hu, and P. C. Painter, *Macromolecules*, **21**, 59 (1988).
11. R. W. Seymour, G. M. Estes, and S. L. Cooper, *Macromolecules*, **3**(5), 579 (1970).
12. G. C. Pimentel and A. L. McClellan, *The Hydrogen Bond*, W. H. Freeman, San Francisco, CA, 1960, p. 136.
13. K. K. S. Hwang, G. Wu, S. B. Lin, and S. L. Cooper, *J. Polym. Sci. Polym. Chem. Ed.*, **22**, 1677 (1984).
14. K. H. Hsieh, C. C. Tsai, and S. M. Tseng, *J. Membr. Sci.*, **49**, 341 (1990).
15. L. D. Landro, M. Pegoraro, and L. Bordogna, *J. Membr. Sci.*, **64**, 229 (1991).
16. R. W. Seymour and S. L. Cooper, *Macromolecules*, **6**(1), 48 (1973).
17. P. D. Nair, M. Jayabalam, and V. N. Krishnamurthy, *J. Polym. Sci. Part A Polym. Chem.*, **28**, 3775 (1990).
18. W. M. Jackson and R. T. Conley, *J. Appl. Polym. Sci.*, **8**, 2163 (1964).
19. W. F. Hale, A. G. Frarnham, R. N. Johnson, and R. A. Clendinning, *J. Polym. Sci. Part A-1*, **5**, 2399 (1967).
20. C. M. Brunette, S. L. Hsu, M. Rossman, W. J. Macknight, and N. S. Schneider, *Polym. Eng. Sci.*, **21**(11), 668 (1981).

Received October 1, 1994

Accepted April 8, 1995